



Benzene-1,3,5-tricarboxylic acid-functionalized MCM-41 as a novel and recoverable hybrid catalyst for expeditious and efficient synthesis of 2,3-dihydroquinazolin-4(1*H*)-ones via one-pot three-component reaction

Niusha Nikooei¹ · Mohammad G. Dekamin¹ · Ehsan Valiey¹

Received: 30 March 2020 / Accepted: 11 May 2020
© Springer Nature B.V. 2020

Abstract

Benzene-1,3,5-tricarboxylic acid-functionalized MCM-41 (MCM-41-Pr-BTA), as a novel hybrid organosilica, was prepared and properly characterized by the Fourier-transform infrared spectroscopy, field emission scanning electron microscopy, transmission electron microscopy, Brunauer–Emmett–Teller, thermal gravimetric analysis and energy-dispersive X-ray spectroscopy to evaluate the functional groups, crystallinity, surface area, morphology, particle size distribution and loading of functional groups. Interestingly, the 1,3-propylene linker used in this study incorporates appropriate catalytic activity into the MCM-41 framework compared to the more known trialkoxypropyl silanes. This new organosilica can be used as a hybrid nanocatalyst for the expeditious and efficient synthesis of 2,3-dihydroquinazolin-4(1*H*)-one derivatives, as an important pharmaceutical scaffold, in aqueous media via a three-component one-pot condensation of isatoic anhydride and aromatic aldehydes with primary amines or ammonium salts. This method has several advantages such as low catalyst loading, high to excellent yields, short reaction times, working under green conditions and simple workup.

Keywords MCM-41 organosilica · Grafting · Mesoporous materials · Hybrid materials · Acid catalysis · Nanoreactor · Heterogeneous catalysis · Green chemistry · Quinazoline derivatives · Ring closure

Electronic supplementary material The online version of this article (<https://doi.org/10.1007/s11164-020-04179-8>) contains supplementary material, which is available to authorized users.

✉ Mohammad G. Dekamin
mdekamin@iust.ac.ir

¹ Pharmaceutical and Heterocyclic Compounds Research Laboratory, Department of Chemistry, Iran University of Science and Technology, Tehran 16846-13114, Iran

Introduction

Heterogeneous catalysis has fascinated greater attention because of easy separation and recyclability. The unique properties of heterogeneous catalysts such as high thermal stability, structural diversity, easy modifications, strong absorption and low toxicity have made them attractive in some industrial applications such as chemical, pharmaceutical, automobile and petrochemical industries [1–6].

One of the best-known support materials having silica structure is mesoporous MCM-41, which has a hexagonal array of one-dimensional pore structures. This mesoporous silica can be obtained by a simple procedure and shows outstanding structural properties with the high specific surface area (up to $2000 \text{ m}^2 \text{ g}^{-1}$) and pore diameter in the range 15–100 Å [7–11]. The acidity of MCM-41 is low. Hence, to overcome this limitation, different methods have been improved to increase their acidity including replacement of Si atoms in the lattice by metal ions including Al, B, Fe and Zr or anchoring suitable organic functional groups [12–16]. The later modification of the MCM texture affords mesoporous organosilicas by post-modification and co-condensation methods as well as periodic mesoporous organosilicas (PMOs) [17–26].

Nowadays, mesoporous organosilicas with unique surface area and porous structure have been developed as the promising candidates in catalysis of various kinds of organic transformations and green chemistry. Indeed, these materials can be prepared with different particle sizes and morphologies. On the other hand, the presence of different functional groups on the surface of silica allows these materials to have diverse tunable physical and chemical properties [27]. Because of their unique structural properties, mesoporous organosilica materials have many applications including catalysis [10, 21, 28], drug delivery [29, 30], CO₂ capture or transformation [31–33], environmental cleanup, separation technology, sensing and optoelectronics [34–36].

Furthermore, one of the environment friendly methods for the synthesis of organic compounds is the use of one-pot multicomponent reactions (MCRs) [28, 37–41]. They can produce the desired products in a single step and also the diversity could be achieved simply by varying the reacting components, which has advantages such as high atom economy, milder reaction conditions, shorter reaction times, lower energy consumption and cost formation of essential carbon–carbon and carbon–heteroatom bonds [13–15, 37, 42–50]. Therefore, MCRs can be considered as an important tool for synthesis of complex organic compounds especially for the synthesis of heterocycles demonstrating bioactive scaffolds [38, 41, 42, 51–58]. Moreover, MCRs that are carried out in water, as a green and the most abundant solvent, address more environmental concerns [47, 50, 59–62]. Indeed, water offers a unique reactivity and selectivity as well as easy separation of the products from the reactions mixtures [16, 63].

Quinazolinones and their oxidation products are fused nitrogen-containing heterocycles with unique pharmaceutical and biological activities [64–69]. For example, 2,3-dihydroquinazolin-4(1*H*)-one derivatives such as A, B and C are valuable compounds as diuretic, antifungal and thermogenic agents, respectively (Fig. 1) [69–71].

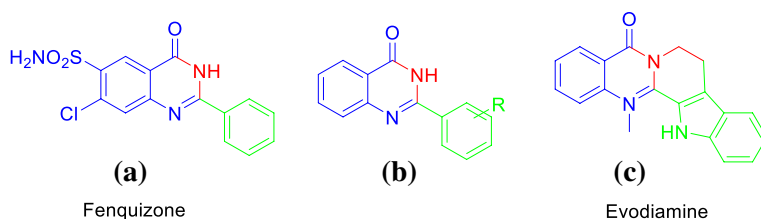
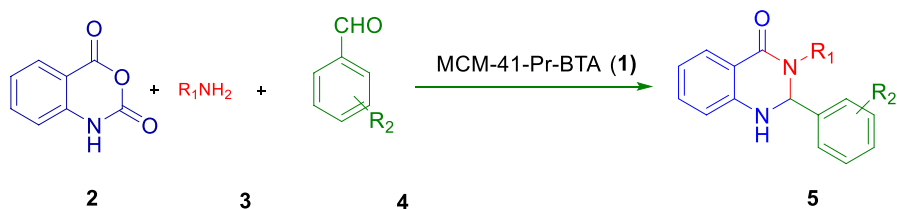


Fig. 1 Selected examples illustrating the medicinal importance of quinazolinones

Due to importance of quinazoline derivatives, different catalytic systems for the synthesis of 2,3-dihydro-4(1*H*)-quinazolinones based on MCR strategy have been developed. Some recent examples include SrCl₂ [72], Zn(PFO)₂ [73], Ga(OTf)₃ [74], I₂ [75], copper-benzenesulfonate [76], aluminum methanesulfonate [77], cation exchange resin [78], *p*-TSA via ball milling [65], starch sulfate [79], silica sulfuric acid [80], silica-bonded S-sulfonic acid [80], PTSA-formaldehyde copolymer [81], β-cyclodextrin-SO₃H [82], magnetic Fe₃O₄ nanoparticles [62], Al/Al₂O₃ nanoparticles [80], CuO nanoparticles using sonication [83], nano-ordered In₂O₃ [84], montmorillonite K-10 [85] and Amberlyst-15 under microwave irradiation [86]. Some of these procedures show some disadvantages such as long reaction times, low yields, harsh reaction conditions and the use of expensive or toxic catalysts. Therefore, to avoid these limitations, the exploration of an efficient, easily available catalyst with high catalytic activity and short reaction times for the preparation of quinazoline derivatives is still in demand. From this point of view, benzene-1,3,5-tricarboxylic acid can be used as a bidentate acidic group for post-modification of the MCM-41 surface to carry out various organic transformations with increased selectivities. We wish herein to disclose the promising catalytic activity of highly ordered mesoporous MCM-41 functionalized with a grafted benzene-1,3,5-tricarboxylic acid through 1,3-propylene linker (MCM-41-Pr-BTA, **1**) for the one-pot three-component reaction of isatoic anhydride (**2**) with diverse amines **3** and aldehydes **4** to afford biologically active quinazoline derivatives **5** (Scheme 1).



Scheme 1 One-pot three-component reaction of isatoic anhydride (**2**) with diverse amines **3** and aldehydes **4** catalyzed by MCM-41-PR-BTA (**1**) for synthesis of quinazoline derivatives **5**

Results and discussion

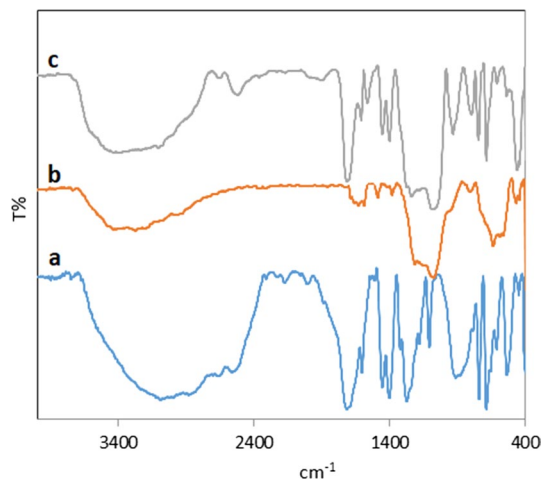
Characterization of the MCM-41-Pr-BTA catalyst (1)

The prepared MCM-41-Pr-BTA nanocatalyst (**1**) was characterized by FT-IR (Fig. 2). The FT-IR spectra of MCM-41 (b) and MCM-41-Pr-BTA (c) show the absorption bands around 806 cm^{-1} , 960 cm^{-1} and 1074 cm^{-1} with a shoulder at $\sim 1070\text{ cm}^{-1}$ which are ascribed to the symmetric stretching of Si–O–Si, Si–OH and the asymmetric stretching of Si–O–Si, respectively. On the other hand, the signal at 1600 is for water absorbed by the surface of MCM-41 (b). Furthermore, the catalyst showed an adsorption band at $1390\text{--}1400\text{ cm}^{-1}$ which is assigned to C=C of the BTA (a, c). Also, the spectrum of the BTA-functionalized MCM-41 (**1**) shows a broadband at $3600\text{--}2400\text{ cm}^{-1}$ for hydroxyls groups of BTA as well as MCM-41. The sharp band at 1715 cm^{-1} was attributed to the carbonyl groups of BTA. By comparing spectra of MCM-41, BTA and MCM-41-Pr-BTA (**1**), it can be concluded that BTA has been successfully grafted on the surface of MCM-41.

Also, the crystallinity and orderliness of the MCM-41-Pr-BTA (**1**) were determined by XRD patterns. The low- and wide-angle XRD patterns for the MCM-41-Pr-BTA are shown in Fig. 3. The peaks located at $2\theta = 2.5^\circ$, 3.5° , 3.8° , 4.5° , 5.7° , 6.3° and 6.6° are typical for the amorphous silica of mesoporous MCM-41, which indicates a hexagonally packed mesoporous structure [87]. Indeed, the peak at 2.5° is the characteristic peak for MCM-41. On the other hand, the wide-angle XRD of MCM-41 usually shows a broad peak in $2\theta = 20^\circ\text{--}30^\circ$. These patterns of the catalyst demonstrate five characteristic peaks at $2\theta = 11^\circ$, 13° , 24° , 27° and 30° , respectively. The reference codes for MCM-41 and 1,3,5-benzenetricarboxylic acid are 00-049-1712 and 00-045-1880, respectively, which are attributed to the presence of these moieties in the structure of MCM-41-Pr-BTA.

FE-SEM analysis was used to determine the surface morphology and particle size distribution for the nanocatalyst (**1**). Figure 4 shows the obtained images for the

Fig. 2 FT-IR spectra of the commercial BTA (a), MCM-41 (b), MCM-41-Pr-BTA (**1**, c)



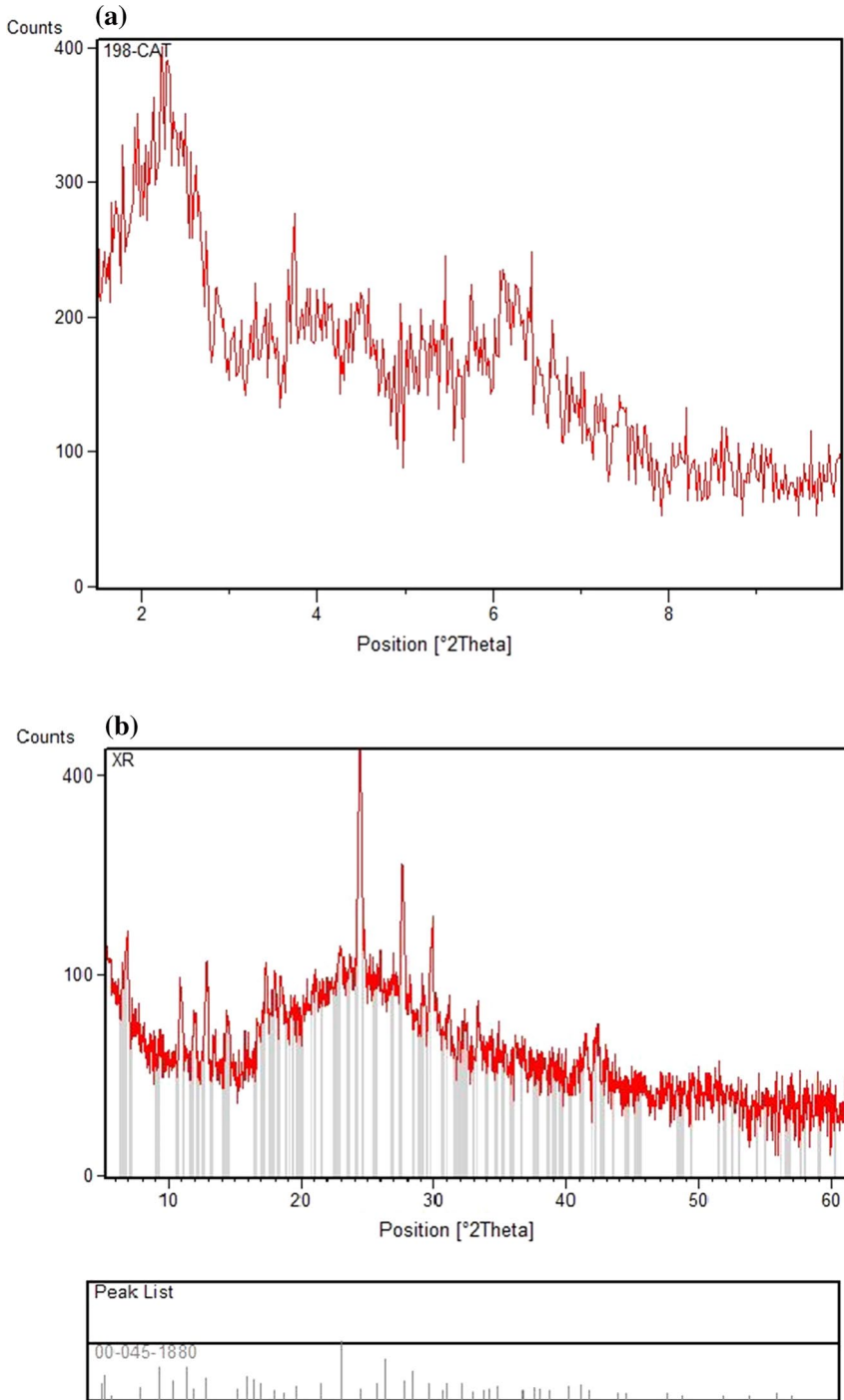
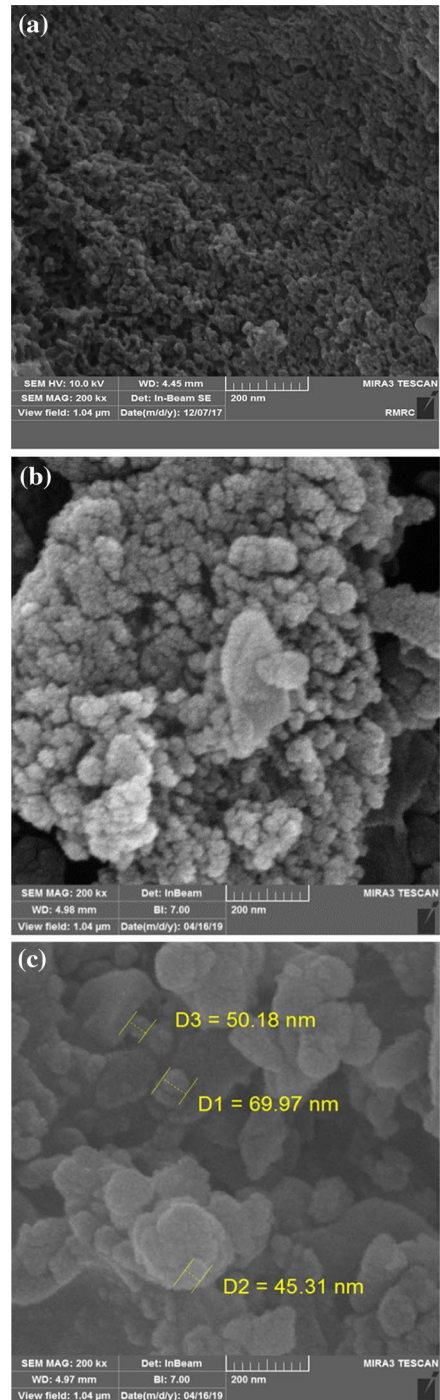


Fig. 3 XRD pattern of the catalyst 1 a low angle, b wide angle

Fig. 4 FE-SEM images of the
a MCM-41 **b, c** MCM-41-Pr-
BTA **1**



MCM-41 before and after grafting of BTA molecules with no significant agglomeration on the surface of the catalyst **1**. By comparing of FE-SEM images, it can be realized that the surface morphology of the MCM-41-Pr-BTA (**1**) is mainly spherical and different from that of the pure MCM-41. Furthermore, it can be concluded that 1,3,5-benzenetricarboxylic acid molecules have been successfully grafted onto the surface of MCM-41.

Moreover, the EDX analysis was used to find the percentage of elements which are present in the structure of both MCM-41 and MCM-41-Pr-BTA (**1**). Figure 5a reveals the existence of only Si and O atoms for MCM-41. On the other hand, the appearance of the C peak proves that both BTA and 1,3-propylene linker have been successfully grafted on the surface of the MCM-41 (Fig. 5b). Indeed, the weight percentage of the elements of Si and O was found to be 32.40 and 67.60, respectively. However, the weight percentage of these elements in the structure of MCM-41-Pr-BTA was 18.14 and 54.11, respectively; meanwhile, the percentage of C was found to be 27.75.

The thermogravimetric analysis (TGA) was used to show the percentage of chemisorbed organic layers onto the surface of mesoporous MCM-41. The TGA curve of MCM-41-Pr-BTA (**1**) shows three-step mass losses (Fig. 6). The first step shows the small amount of weight loss about 5% below 200 °C which is due to the desorption of physically adsorbed water and organic solvents. The second one occurred between 300 and 400 °C, which was assigned to the decomposition of covalently bonded organics (4% weight loss). The third step of mass loss was about 2% between 400 and 500 °C which may be attributed to the thermal dehydration of silanol groups to the siloxane ones [33].

On the other hand, the specific surface area of the MCM-41-Pr-BTA mesoporous catalyst (**1**) was measured by Brunauer, Emmett and Teller (BET) method. The N₂ sorption isotherms of MCM-41-Pr-BTA are illustrated in Fig. 7. Based on the IUPAC classification, the catalyst **1** exhibits a type IV isotherm with H₂ hysteresis loop which is characteristic of the typical of mesoporous materials. The analysis for the final catalyst **1** and its precursor materials are reported in Table 1. The observed decrease in the BET surface area, pore volume and pore size could be attributed to the covalent bonding of organic BTA and 1,3-propylene linker on the surface of MCM-41 channels.

Investigation of the catalytic activity of mesoporous MCM-41-Pr-BTA for three-component 2,3-dihydroquinazolin-4(1H)-one derivatives

After the characterization of the catalyst **1**, the three-component reaction of isoatoic anhydride (**2**) with ammonium acetate (**3a**) and 4-chlorobenzaldehyde (**4a**) was chosen as the model reaction. Then, the effect of different temperatures and solvents was systemically studied on the progress of model reaction with various loadings of MCM-41-Pr-BTA (**1**) as the catalyst. The results are summarized in Table 2. The amount of the catalyst **1** played an important role in the model reaction. Indeed, the reaction in the absence of the MCM-41-Pr-BTA affords a poor yield of the desired 2-(4-chlorophenyl)-2,3-dihydroquinazolin-4(1H)-one (**5a**) after 24 h under

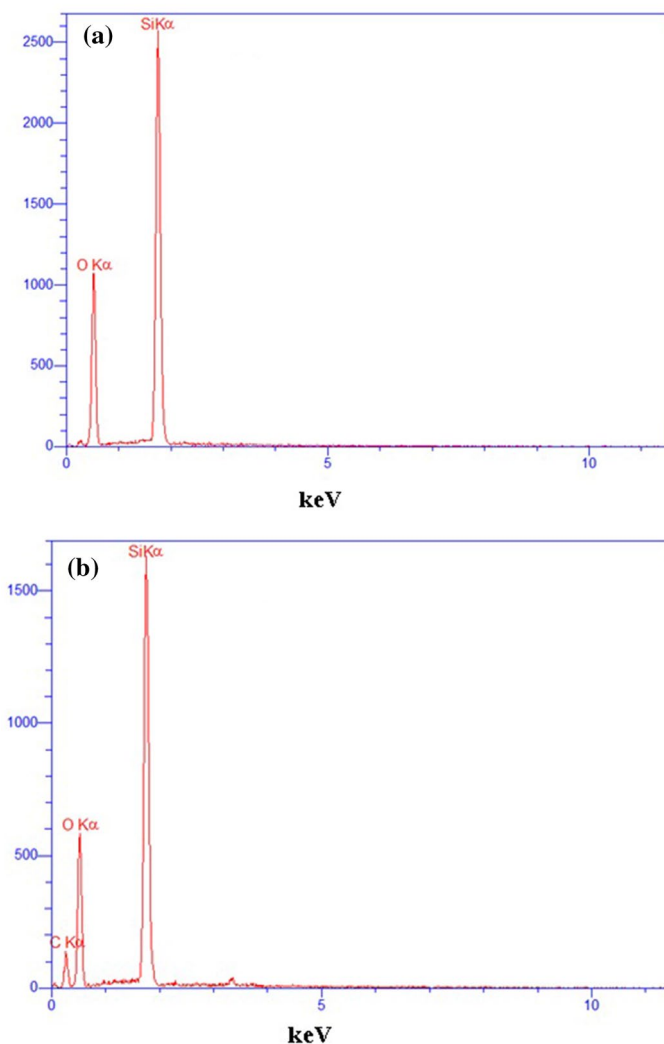


Fig. 5 Energy-dispersive X-ray (EDX) spectroscopy pattern of **a** MCM-41, **b** catalyst (**1**)

reflux conditions (entry 1, Table 2). As can be seen in Table 2, adding 0.01 g of the mesoporous hybrid catalyst **1** did significantly improve the yield of the desired product **5a** (entries 2–4). The highest yield of the desired product **5a** was obtained by 0.01 g catalyst in H₂O under reflux conditions (entry 4, Table 2). On the other hand, the effect of sonication was also studied under the same conditions (entries 4, 5). In our hands, classical heating afforded better yield than ultrasonic conditions. The same result was obtained in water at room temperature (entry 6, Table 2). Moreover, the effect of other solvents including MeOH, MeCN, CH₂Cl₂, THF and toluene was also studied on the progress of the model reaction under same catalyst loading (entries 7–11). Consequently, among all the solvents screened water was selected as

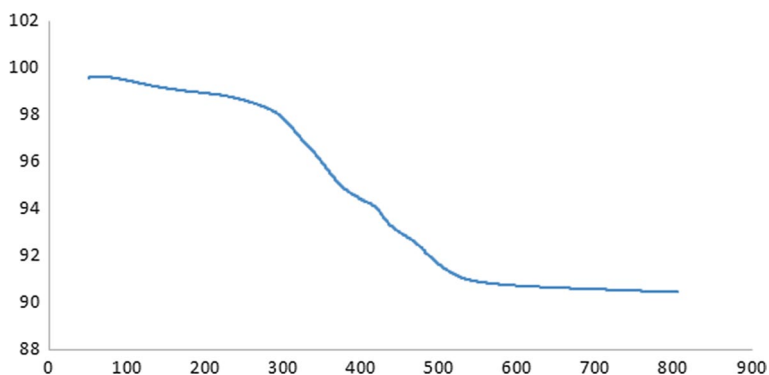


Fig. 6 TGA of the MCM-41-Pr-BTA (1)

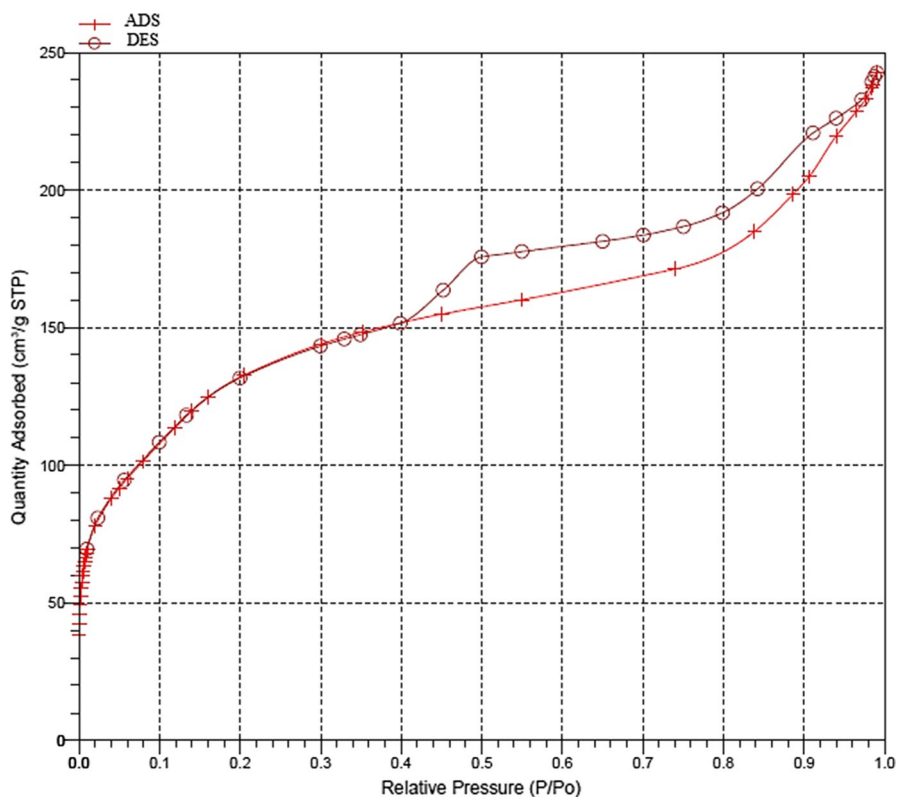
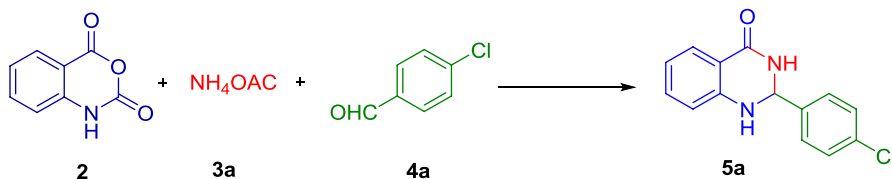


Fig. 7 Adsorption/desorption isotherms of the MCM-41-Pr-BTA (1)

the optimal solvent in next experiments. The effect of lower catalyst loadings than 0.01 g was further studied (entries 13–15). Moderate yields of the desired product **5a** were obtained in all studied cases.

Table 1 Textural parameters of the MCM-41 and MCM-41-Pr-BTA (**1**) samples

| Samples | BET surface area (m ² /g) | Total pore vol. (cm ³ /g) ($p/p_0=0.98$) | Pore size (nm) |
|----------------------------|--------------------------------------|---|----------------|
| MCM-41 [16] | 926 | 1.09 | 4.07 |
| MCM-41-Pr-BTA (1) | 435 | 0.36 | 3.37 |

Table 2 Optimization of the three-component reaction of isatoic anhydride (**2**) with ammonium acetate (**3a**) and 4-chlorobenzaldehyde (**4a**) under various conditions.^a

| Entry | Catalyst loading (g) | Solvent | Temperature (°C) | Time (min) | Yield ^b (%) |
|-------|----------------------|---------------------------------|------------------|------------|------------------------|
| 1 | – | EtOH | Reflux | 24 h | Trace |
| 2 | 0.01 | EtOH | Reflux | 55 | 82 |
| 3 | 0.01 | H ₂ O/EtOH (1:1) | Reflux | 35 | 78 |
| 4 | 0.01 | H ₂ O | Reflux | 15 | 92 |
| 5 | 0.01 | H ₂ O | Ultrasonic | 60 | 40 |
| 6 | 0.01 | H ₂ O | r.t. | 75 | 53 |
| 7 | 0.01 | MeOH | Reflux | 30 | 75 |
| 8 | 0.01 | MeCN | Reflux | 45 | 55 |
| 9 | 0.01 | Toluene | Reflux | 40 | 45 |
| 10 | 0.01 | CH ₂ Cl ₂ | Reflux | 30 | 52 |
| 11 | 0.01 | THF | Reflux | 100 | 35 |
| 12 | 0.01 | – | 100 | 135 | 71 |
| 13 | 0.007 | H ₂ O | Reflux | 25 | 79 |
| 14 | 0.005 | H ₂ O | Reflux | 40 | 60 |
| 15 | 0.003 | H ₂ O | Reflux | 50 | 55 |

^aReaction conditions: isatoic anhydride (**2**, 1 mmol), ammonium acetate (**3a**, 1.2 mmol), 4-chlorobenzaldehyde (**4a**, 1 mmol), MCM-41-Pr-BTA (**1**) and solvent (2 mL). ^bIsolated yields

The optimized conditions were developed to other aromatic aldehydes **4a–j** or amine sources **3a–c**, in the next step of study. The obtained results are summarized in Tables 3 and 4, respectively. Indeed, all the studied aldehydes or amine sources were involved in the optimized conditions to afford a wide range of pharmaceutically active products **5–7** in high to excellent yields. From data provided in Tables 3 and 4 condensation of ammonium acetate (**3a**) or aniline derivatives **3b–c** with aromatic aldehydes **4**, it can be concluded that aldehydes having electron-withdrawing

substituents produced corresponding quinazoline derivatives **5–7** in shorter reaction times or higher yields than aldehydes bearing electron-donating ones.

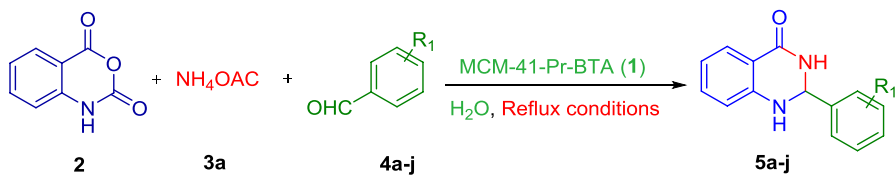
According to the obtained results, a plausible mechanism can be proposed for the synthesis of 2,3-dihydroquinazolin-4(1*H*)-ones **5–7** from condensation of isatoic anhydride (**2**) with different amine sources **3a–c** and aldehydes **4** in the presence of MCM-41-Pr-BTA mesoporous hybrid catalyst **1** (Scheme 2). First, the isatoic anhydride (**2**) is activated by MCM-41-Pr-BTA (**1**) for nucleophilic addition of the amine sources **3a–c** to afford intermediate (**III**) through intermediates (**I**) and (**II**) with CO₂ elimination. Then, the *N*-nucleophilic amine attack of anthranilamide (**III**) on the activated carbonyl functional group of aldehydes **4** produces iminium intermediate (**V**) with losing of H₂O. Subsequently, intramolecular nucleophilic attack of the amide nitrogen to the activated imine moiety produces heteroannulated products **5–7**.

One of the advantages of heterogeneous catalysts is their easy separation from the reaction mixture and subsequent reusing in catalytic systems. Therefore, the reusability can be very important in industry. In this part of our study, the reusability of MCM-41-Pr-BTA (**1**) was investigated in the model reaction for further runs. After completion of the reaction indicated in Table 3, the nanocatalyst was removed by filtration from the reaction mixture and washed with EtOH, EtOAc and *n*-hexane, respectively. Then, it was dried in an oven at 70 °C for 1 h. The recycled catalyst **1** was used again in the model reaction. To our delight, the reaction yield did not change significantly after five consecutive runs and a little loss of catalytic activity of these new heterogeneous catalyst was observed (Fig. 8).

Finally, the efficiency of nanomaterial **1** was compared with some different reported catalytic systems for the synthesis of 2-(4-chlorophenyl)-2,3-dihydroquinazolin-4(1*H*)-one (**5a**) and the results are listed in Table 5. As data provided in Table 5 demonstrate, the hybrid organocatalyst **1** gives better yield in shorter reaction times than the compared catalysts. Interestingly, the 1,3-propylene linker used in this study incorporates appropriate catalytic activity into the MCM-41 framework compared to the more known trialkoxypropyl silanes.

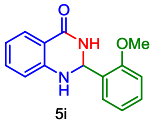
Conclusions

In summary, we have employed an effective and practical procedure for the synthesis of 2,3-dihydroquinazolin-4(1*H*)-ones derivatives via the one-pot three-component condensation of isatoic anhydride, aromatic aldehyde and amine using catalytic amount of MCM-41-Pr-BTA under reflux conditions. The hybrid organosilica nanocatalyst is highly efficient, easily prepared from commercially available precursors and non-toxic. The other attractive features of this new methodology are low loading transition metal-free catalyst, high to excellent yields, facile workup environmentally friendly procedure, mild conditions and short reaction times.

Table 3 MCM-41-Pr-BTA (**1**)-catalyzed synthesis of 2,3-dihydroquinazolin-4(1*H*)-ones **5** under optimized conditions^a

| Entry | Aldehyde 4 | Product | Time (min) | Yield ^b (%) | Mp (°C) found | Mp (°C) reported |
|-------|------------|---------|------------|------------------------|---------------|------------------|
| 1 | | | 15 | 92 | 200–210 | 198–200 [78] |
| 2 | | | 25 | 88 | 189–193 | 192–193 [88] |
| 3 | | | 20 | 86 | 232–235 | 233–234 [89] |
| 4 | | | 15 | 90 | 197–200 | 199–200 [74] |
| 5 | | | 18 | 93 | 352–350 | 351–352 [74] |
| 6 | | | 15 | 85 | 210–214 | 213–214 [74] |
| 7 | | | 20 | 84 | 215–220 | 216–217 [74] |
| 8 | | | 20 | 94 | 200–204 | 202–204 [78] |

Table 3 (continued)

| Entry | Aldehyde 4 | Product | Time (min) | Yield ^b (%) | Mp (°C) found | Mp (°C) reported |
|-------|---|---|------------|------------------------|---------------|------------------|
| 9 |  |  | 27 | 86 | 165–167 | 165–167 [79] |
| 10 |  |  | 20 | 87 | 218–220 | 218–220 [90] |

^aReaction conditions: isatoic anhydride (**2**, 1 mmol), ammonium acetate (**3a**, 1.2 mmol), 4-chlorobenzaldehyde (**4a**, 1 mmol), MCM-41-Pr-BTA (**1**) in H₂O (2 mL) under reflux conditions. ^bIsolated yields

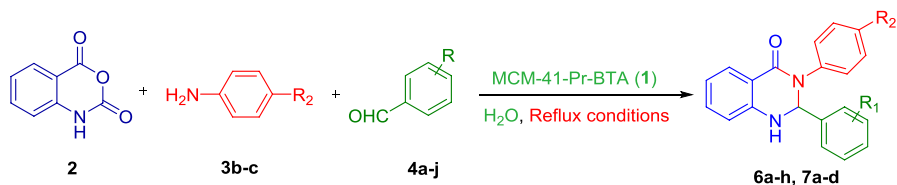
Experimental section

Reagents and apparatus

All chemicals and reagents were purchased from Merck and Aldrich and used without further purification, except for aniline and benzaldehyde, for which fresh distilled samples were used. FT-IR spectra were recorded as KBr pellets on a Shimadzu FT-IR-8400S spectrometer. All diffuse reflectance spectra were recorded at room temperature against KBr and were plotted in terms of absorbance. ¹H NMR (500 MHz) spectra were obtained using a Bruker DRX-500 Avance spectrometer. All ¹H NMR spectra were run in CDCl₃ solution, relative to TMS (0.00 ppm), at ambient temperature. Melting points were determined using an Electrothermal 9100 apparatus and uncorrected. MCM-41 and MCM-41-Pr-Br materials were prepared according to our previously reported procedure and characterized by FT-IR spectroscopy [16]. All products were characterized by spectroscopic methods (IR and ¹H NMR spectra) and melting points.

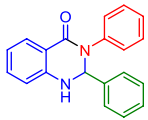
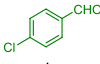
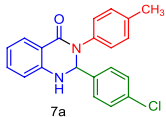
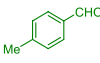
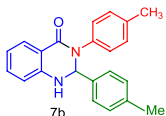
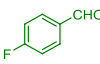
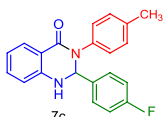
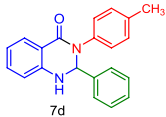
Preparation of the MCM-41-Pr-BTA

The mesoporous silica (MCM-41, 0.2 g) was suspended in toluene (20 ml), and 1 g 1,3-dibromopropane was added to the obtained mixture at room temperature and stirred for 24 h. After that, the obtained white solids were filtered and washed with toluene (2.5 ml) and EtOH (2.5 ml), respectively, and dried in an oven to afford MCM-41-Pr-Br. After that, 0.1 g MCM-41-Pr-Br and 0.01 g KI were suspended in DMSO (30 ml) and stirred for 10 h at room temperature. Then, 1,3,5-benzenetricarboxylic acid (BTA, 0.1 g) and K₂CO₃ (0.055 g) were added to the obtained mixture and stirred for 1 h. Finally, the obtained white solids of the catalyst **1** were filtered, washed with H₂O (2.5 ml) and EtOH (2.5 ml) and dried in an oven.

Table 4 MCM-41-Pr-BTA (**1**) catalyzed reaction between isatoic anhydride (**2**), aniline (**3b**) or *p*-toluidine (**3c**) and aromatic aldehydes (**4a–h**) under optimized conditions^a

| Entry | Aldehyde | Product | Time (min) | Yield (%) | Mp (°C) found | Mp (°C) reported ^[lit.] |
|-------|----------|---------|------------|-----------|---------------|------------------------------------|
| 1 | | | 25 | 90 | 213–215 | 214–217 [61] |
| 2 | | | 35 | 86 | 200–204 | 204–205 [73] |
| 3 | | | 30 | 80 | 214–216 | 215–216 [62] |
| 4 | | | 28 | 87 | 232–236 | 235–238 [91] |
| 5 | | | 30 | 81 | 194–196 | 194–196 [73] |
| 6 | | | 35 | 79 | 185–188 | 186–188 [92] |
| 7 | | | 40 | 86 | 200–215 | 212–214 [72] |

Table 4 (continued)

| Entry | Aldehyde | Product | Time (min) | Yield (%) | Mp (°C) found | Mp (°C) reported ^[lit.] |
|-------|---|---|------------|-----------|---------------|------------------------------------|
| 8 |  4j |  6h | 25 | 85 | 200–215 | 214–215 [74] |
| 9 |  4a |  7a | 20 | 87 | 250–252 | 250–252 [74] |
| 10 |  4a |  7b | 25 | 83 | 240–245 | 243–246 [74] |
| 11 |  4d |  7c | 23 | 86 | 240–245 | 241–243 [62] |
| 12 |  4j |  7d | 30 | 81 | 195–200 | 197–198 [62] |

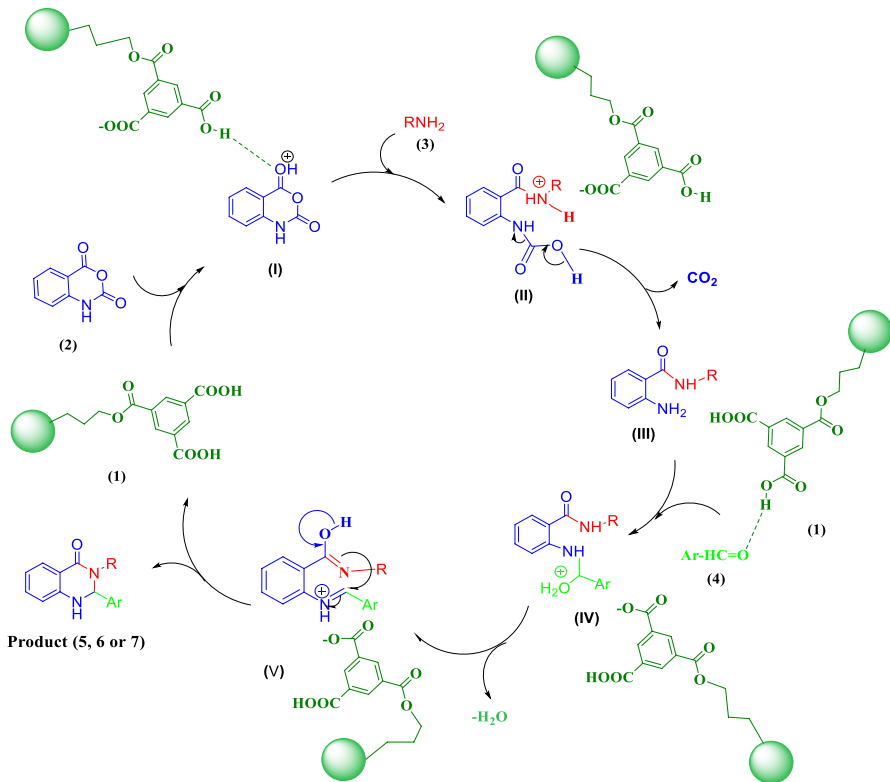
^aReaction conditions: Isatoic anhydride (**2**, 1 mmol), ammonium acetate (**3a**, 1.2 mmol), 4-chlorobenzaldehyde (**4a**, 1 mmol), MCM-41-Pr-BTA (**1**) in H₂O (2 mL) under reflux conditions. ^bIsolated yields

Typical procedure for the one-pot synthesis of 2,3-dihydroquinazolin-4(1H)-ones

MCM-41-Pr-BTA (0.01 g) was added to a mixture of isatoic anhydride (**2**, 1.0 mmol, 0.163 g), primary amine or ammonium acetate (**3**, 1.2 mmol) and aryl aldehydes (**4**, 1.0 mmol) in 2 ml of distilled water, and the obtained mixture was stirred under reflux conditions for the appropriate times indicated in Table 2. The reaction progress was monitored by TLC (eluent: *n*-hexane/EtOAc, 3:1). After completion of the reaction, the solvent was evaporated; then, hot EtOH was added to the mixture and the catalyst was separated by filtration. *n*-Hexane was then added to the filtrate dropwise and allowed to cool over time to give pure crystals of the desired 2,3-dihydroquinazolin-4(1H)-one derivatives.

Selected Spectral Data

2-(2-Chlorophenyl)-3-phenyl-2,3-dihydroquinazolin-4(1H)-one (6 g) White solid, Mp: 200–215 °C. ¹HNMR (500 MHz, DMSO-d₆): δ (ppm) 6.6 (d, *J* = 6.2 Hz, 1H), 6.7



Scheme 2 Proposed mechanism of synthesis of 2,3-dihydroquinazolin-4(1H)-ones of MCM-41-Pr-BTA mesoporous hybrid catalyst **1**

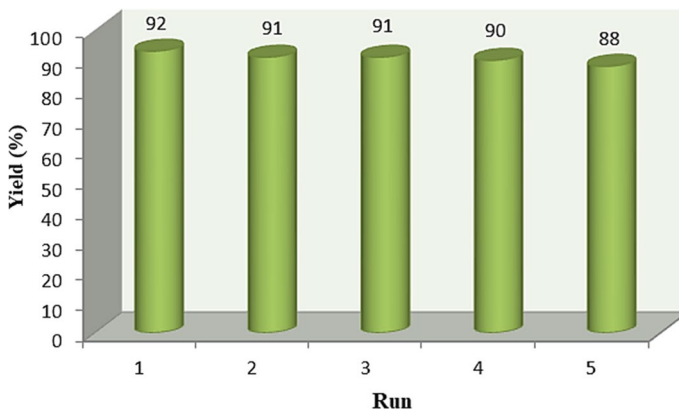


Fig. 8 Reusability of the nanocatalyst **1** in five consecutive runs for the synthesis of **5a**

Table 5 Comparative synthesis of compound **5a** using the reported heterogeneous catalysts versus the present method

| Entry | Catalyst | Product | Catalyst loading | Conditions | Time (min) | Yield (%) | References |
|-------|-----------------------|-----------|------------------|-----------------------------------|------------|-----------|------------|
| 1 | Nano-ZnO | 4a | 20 mol% | Solvent free | 180 | 80 | [83] |
| 2 | Silica sulfuric acid | 4a | 20 mol% | Solvent free | 300 | 80 | [83] |
| 3 | Oxalic acid | 4a | 20 mol% | EtOH/ H ₂ O1:1(v/v) | 40 | 90 | [93] |
| 4 | β -Cyclodextrin | 4a | 0.2 mol% | Reflux H ₂ O | 180 | 84 | [74] |
| 5 | Al-SBA-15 | 4a | 0.03 g | Reflux EtOH | 45 | 80 | [94] |
| 6 | MCM-41 | 4a | 0.01 g | Reflux H ₂ O | 120 | 67 | This work |
| 7 | MCM-41-PR-BTA | 4a | 0.01 g | Reflux H ₂ O | 15 | 92 | This work |
| 8 | BTA | 4a | 0.01 g | Reflux H ₂ O | 45 | 60 | This work |

(q, 2H), 7.2 (m, 3H), 7.3 (m, 5H), 7.4 (m, 1H), 7.5 (d, $J=8.7$ Hz, 1H), 7.6 (m, 1H), 7.7 (d, $J=7.9$ Hz, 1H); IR (KBr) max (cm⁻¹): 3292, 3028, 1631, 1487.

2-(2-Chlorophenyl)-2,3-dihydroquinazolin-4(1H)-one (5 h) White solid, Mp: 200–204 °C. ¹H NMR (500 MHz, DMSO-d₆): δ (ppm) 6.1 (s, 1H), 6.7 (t, 1H, $J=6.7$ Hz), 6.8 (d, 1H, $J=7.6$ Hz), 7.02 (s, 1H), 7.2 (m, 4H), 7.4 (m, 3H), 7.6 (d, 2H, $J=4.3$ Hz), 8.2 (s, 1H); IR (KBr) max (cm⁻¹): 3303, 3174, 3033, 1654, 1483, 1481.

2-(4-Methylphenyl)-2,3-dihydroquinazolin-4(1H)-one (5c) White solid, Mp: 189–193 °C. ¹H NMR (500 MHz, DMSO-d₆): δ (ppm) 8.2 (s, 1H), 7.6 (d, $J=8.3$ Hz, 1H), 7.3 (d, 2H, $J=7.9$ Hz), 7.2 (doublet of triplet, 1H, $J=8.1$), 7.1 (d, $J=7.7$ Hz, 2H), 7.0 (s, 1H), 6.7 (d, 1H, $J=7.9$ Hz), 6.6 (m, 1H), 5.7 (s, 1H), 2.3 (s, 3H); IR (KBr) max (cm⁻¹): 3290, 3164, 3024, 2929, 2821, 1500, 1250.

Acknowledgements The financial support from The Research Council of Iran University of Science and Technology (IUST), Tehran, Iran (Grant No: 160/18517), is highly appreciated. The partial financial support of The Iran Nanotechnology Initiative Council (INIC) is gratefully acknowledged.

References

1. L. Liu, A. Corma, Chem. Rev. **118**, 4981 (2018)
2. V. Polshettiwar, R.S. Varma, Green Chem. **12**, 743 (2010)
3. M.S. Azam, C. Cai, J.M. Gibbs, E. Tyrode, D.K. Hore, J. Am. Chem. Soc. **142**, 669 (2020)
4. T. Rahman, G. Borah, P.K. Gogoi, Catal. Lett. (2020). <https://doi.org/10.1007/s10562-020-03131-0>
5. Y. Wang, J. Wang, Y. Zhang, F. Song, Y. Xie, M. Wang, H. Cui, W. Yi, Catal. Lett. **150**, 493 (2020)
6. A. Azad, M.G. Dekamin, S. Afshar, A. Tadjarodi, A. Mollahosseini, Res. Chem. Intermed. **44**, 2951 (2018)
7. S. Rojas-Buzo, P. García-García, A. Corma, Catal. Sci. Technol. **9**, 146 (2019)

8. M. Eslami, M.G. Dekamin, L. Motlagh, A. Maleki, *Green Chem. Lett. Rev.* **11**, 36 (2018)
9. J. Chun, Y.M. Gu, J. Hwang, K.K. Oh, J.H. Lee, *J. Ind. Eng. Chem.* **81**, 135 (2020)
10. D.E. De Vos, M. Dams, B.F. Sels, P.A. Jacobs, *Chem. Rev.* **102**, 3615 (2002)
11. S.N. Jadhav, S.P. Patil, D.P. Sahoo, D. Rath, K. Parida, C.V. Rode, *Catal. Lett.* (2020). <https://doi.org/10.1007/s10562-019-03089-8>
12. M. Xu, W. Wang, M. Seiler, A. Buchholz, M. Hunger, *J. Phys. Chem. B* **106**, 3202 (2002)
13. M.G. Dekamin, Z. Mokhtari, *Tetrahedron* **68**, 922 (2012)
14. A.A. Amiri, S. Javanshir, Z. Dolatkah, M.G. Dekamin, *New J. Chem.* **39**, 9665 (2015)
15. K. Iwanami, H. Seo, J.-C. Choi, T. Sakakura, H. Yasuda, *Tetrahedron* **66**, 1898 (2010)
16. Z. Alirezvani, M.G. Dekamin, E. Valiey, *ACS Omega* **4**, 20618 (2019)
17. J.C. Manayil, A.F. Lee, K. Wilson, *Molecules* **24**, 239 (2019)
18. P. Van Der Voort, D. Esquivel, E. De Canck, F. Goethals, I. Van Driessche, F.J. Romero-Salguero, *Chem. Soc. Rev.* **42**, 3913 (2013)
19. M. Waki, N. Mizoshita, T. Tani, S. Inagaki, *Angew. Chem. Int. Ed.* **50**, 11667 (2011)
20. S.S. Park, C.S. Ha, *Chem. Rec.* **6**, 32 (2006)
21. Q. Yang, J. Liu, L. Zhang, C. Li, *J. Mater. Chem.* **19**, 1945 (2009)
22. A. Yaghoubi, M.G. Dekamin, E. Arefi, B. Karimi, *J. Colloid Interface Sci.* **505**, 956 (2017)
23. M.G. Dekamin, E. Arefi, A. Yaghoubi, *RSC Adv.* **6**, 86982 (2016)
24. A. Yaghoubi, M.G. Dekamin, B. Karimi, *Catal. Lett.* **147**, 2656 (2017)
25. A. Yaghoubi, M.G. Dekamin, *Chem. Sel.* **2**, 9236 (2017)
26. P. Iliade, I. Miletto, S. Coluccia, G. Berlier, *Res. Chem. Intermed.* **38**, 785 (2012)
27. M.P. Kapoor, S. Inagaki, S. Ikeda, K. Kakiuchi, M. Suda, T. Shimada, *J. Am. Chem. Soc.* **127**, 8174 (2005)
28. A. Kohzadian, H. Filian, Z. Kordrostami, A. Zare, A. Ghorbani-Choghamarani, *Res. Chem. Intermed.* **46**, 1941 (2020)
29. J.-N. Liu, W. Bu, J. Shi, *Chem. Rev.* **117**, 6160 (2017)
30. M. Delle Piane, M. Corno, A. Pedone, R. Dovesi, P. Ugliengo, *J. Phys. Chem. C* **118**, 26737 (2014)
31. M. Ferré, R. Pleixats, M.W.C. Man, X. Cattoën, *Green Chem.* **18**, 881 (2016)
32. S. Loganathan, M. Tikmani, A.K. Ghoshal, *Langmuir* **29**, 3491 (2013)
33. N. Rao, M. Wang, Z. Shang, Y. Hou, G. Fan, J. Li, *Energy Fuels* **32**, 670 (2018)
34. N. Moitra, S. Ichii, T. Kamei, K. Kanamori, Y. Zhu, K. Takeda, K. Nakanishi, T. Shimada, *J. Am. Chem. Soc.* **136**, 11570 (2014)
35. Y. Shu, Y. Shao, X. Wei, X. Wang, Q. Sun, Q. Zhang, L. Li, *Microporous Mesoporous Mater.* **214**, 88–94 (2015)
36. L. Lv, K. Wang, X. Zhao, *J. Colloid Interface Sci.* **305**, 218 (2007)
37. C.G. Neochoritis, T. Zhao, A. Dömling, *Chem. Rev.* **119**, 1970 (2019)
38. A. Dömling, W. Wang, K. Wang, *Chem. Rev.* **112**, 3083 (2012)
39. B. Ganem, *Acc. Chem. Res.* **42**, 463 (2009)
40. X. Xiong, C. Yi, X. Liao, S. Lai, *Catal. Lett.* **149**, 1690 (2019)
41. M. Rimaz, H. Mousavi, L. Ozzar, B. Khalili, *Res. Chem. Intermed.* **45**, 2673 (2019)
42. J.D. Sunderhaus, C. Dockendorff, S.F. Martin, *Org. Lett.* **9**, 4223 (2007)
43. D.J. Ramón, M. Yus, *Angew. Chem. Int. Ed.* **44**, 1602 (2005)
44. H. Eckert, *Molecules* **22**, 349 (2017)
45. Z.-L. Shen, X.-P. Xu, S.-J. Ji, *J. Org. Chem.* **75**, 1162 (2010)
46. J.-T. Li, Y. Yin, M.-X. Sun, *Ultrason. Sonochem.* **17**, 363 (2010)
47. M.C. Pirrung, K.D. Sarma, *J. Am. Chem. Soc.* **126**, 444 (2004)
48. M.G. Dekamin, M. Azimoshan, L. Ramezani, *Green Chem.* **15**, 811 (2013)
49. M.G. Dekamin, M. Eslami, *Green Chem.* **16**, 4914 (2014)
50. M.G. Dekamin, M. Eslami, A. Maleki, *Tetrahedron* **69**, 1074 (2013)
51. L. Ma, Y. Qiu, M. Li, D. Cui, S. Zhang, D. Zeng, R. Xiao, *Ind. Eng. Chem. Res.* **59**, 6924 (2020)
52. S. Ilkhanizadeh, J. Khalafy, M.G. Dekamin, *Int. J. Biol. Macromol.* **140**, 605 (2019)
53. F. Davoodi, M.G. Dekamin, Z. Alirezvani, *Appl. Organomet. Chem.* **33**, e4735 (2019)
54. M.G. Dekamin, Z. Karimi, Z. Latifidoost, S. Ilkhanizadeh, H. Daemi, M.R. Naimi-Jamal, M. Barikani, *Int. J. Biol. Macromol.* **108**, 1273 (2018)
55. M.G. Dekamin, F. Mehdipoor, A. Yaghoubi, *New J. Chem.* **41**, 6893 (2017)
56. M.G. Dekamin, E. Kazemi, Z. Karimi, M. Mohammadalipoor, M.R. Naimi-Jamal, *Int. J. Biol. Macromol.* **93**, 767 (2016)
57. Z. Alirezvani, M.G. Dekamin, E. Valiey, *Sci. Rep.* **9**, 17758 (2019)

58. M.G. Dekamin, S.Z. Peyman, Z. Karimi, S. Javanshir, M.R. Naimi-Jamal, M. Barikani, *Int. J. Biol. Macromol.* **87**, 172 (2016)
59. R.A. Sheldon, *Green Chem.* **7**, 267 (2005)
60. A. Chanda, V.V. Fokin, *Chem. Rev.* **109**, 725 (2009)
61. J. Chen, W. Su, H. Wu, M. Liu, C. Jin, *Green Chem.* **9**, 972 (2007)
62. Z.-H. Zhang, H.-Y. Lü, S.-H. Yang, J.-W. Gao, *J. Comb. Chem.* **12**, 643 (2010)
63. H.C. Hailes, *Org. Process Res. Dev.* **11**, 114 (2007)
64. B. Eftekhari-Sis, M. Zirak, *Chem. Rev.* **115**, 151 (2015)
65. G. Yashwantrao, V.P. Jejurkar, R. Kshatriya, S. Saha, *ACS Sustain. Chem. Eng.* **7**, 13551 (2019)
66. P. Kundu, A. Mondal, C. Chowdhury, *J. Org. Chem.* **81**, 6596 (2016)
67. G.M. Chinigo, M. Paige, S. Grindrod, E. Hamel, S. Dakshanamurthy, M. Chruszcz, W. Minor, *M.L. Brown, J. Med. Chem.* **51**, 4620 (2008)
68. A.K. Nanda, S. Ganguli, R. Chakraborty, *Molecules* **12**, 2413 (2007)
69. M. Badolato, F. Aiello, N. Neamati, *RSC Adv.* **8**, 20894 (2018)
70. M.-J. Hour, L.-J. Huang, S.-C. Kuo, Y. Xia, K. Bastow, Y. Nakanishi, E. Hamel, K.-H. Lee, *J. Med. Chem.* **43**, 4479 (2000)
71. M. Bakavoli, O. Sabzevari, M. Rahimizadeh, *Chin. Chem. Lett.* **18**, 1466 (2007)
72. M. Wang, T.T. Zhang, Y. Liang, J.J. Gao, *Chin. Chem. Lett.* **22**, 1423 (2011)
73. L.-M. Wang, L. Hu, J.-H. Shao, J. Yu, L. Zhang, *J. Fluor. Chem.* **129**, 1139 (2008)
74. J. Chen, D. Wu, F. He, M. Liu, H. Wu, J. Ding, W. Su, *Tetrahedron Lett.* **49**, 3814 (2008)
75. S.B. Azimi, J. Azizian, *Tetrahedron Lett.* **57**, 181 (2016)
76. M. Wang, T.T. Zhang, Y. Liang, J.J. Gao, *Monatshefte für Chemie-Chemical Monthly* **143**, 835 (2012)
77. Z. Song, L. Liu, Y. Wang, X. Sun, *Res. Chem. Intermed.* **38**, 1091 (2012)
78. M. Wang, T. Zhang, J. Gao, Y. Liang, *Chem. Heterocycl. Compd.* **48**, 897 (2012)
79. H.R. Shaterian, F. Rigi, *Res. Chem. Intermed.* **41**, 721 (2015)
80. Á. Magyar, Z. Hell, *Catal. Lett.* **146**, 1153 (2016)
81. F. Havasi, A. Ghorbani-Choghamarani, F. Nikpour, *Microporous Mesoporous Mater.* **224**, 26 (2016)
82. F.S. Toosi, M. Khakzadi, *Res. Chem. Intermed.* **41**, 311 (2015)
83. J. Zhang, D. Ren, Y. Ma, W. Wang, H. Wu, *Tetrahedron* **70**, 5274 (2014)
84. S.Y. Abbas, K.A. El-Bayouki, W.M. Basyouni, *Synth. Commun.* **46**, 993 (2016)
85. P. Salehi, M. Dabiri, M. Baghbanzadeh, M. Bahramnejad, *Synth. Commun.* **36**, 2287 (2006)
86. M.P. Surpur, P.R. Singh, S.B. Patil, S.D. Samant, *Synth. Commun.* **37**, 1965 (2007)
87. L. Rout, A. Mohan, A.M. Thomas, C.-S. Ha, *Microporous Mesoporous Mater.* **291**, 109711 (2020)
88. P. Salehi, M. Dabiri, M.A. Zolfigol, M. Baghbanzadeh, *Synlett* **2005**, 1155 (2005)
89. H.L. Yale, M. Kalkstein, *J. Med. Chem.* **10**, 334 (1967)
90. N. Razavi, B. Akhlaghinia, *New J. Chem.* **40**, 447 (2016)
91. C.L. Yoo, J.C. Fettinger, M.J. Kurth, *J. Org. Chem.* **70**, 6941 (2005)
92. A.H. Romero, J. Salazar, S.E. López, *Synthesis* **45**, 2043 (2013)
93. M. Dabiri, P. Salehi, M. Baghbanzadeh, M.A. Zolfigol, M. Agheb, S. Heydari, *Catal. Commun.* **9**, 785 (2008)
94. S. Santra, M. Rahman, A. Roy, A. Majee, A. Hajra, *Catal. Commun.* **49**, 52 (2014)

Publisher's Note Springer Nature remains neutral with regard to jurisdictional claims in published maps and institutional affiliations.